

Atomization and Particle-Jet Interactions in the Wire-Arc Spraying Process

N.A. Hussary and J.V.R. Heberlein

(Submitted 11 August 2000; in revised form 28 November 2000)

The wire-arc spraying process, one of several thermal spray processes, has gained a sizable part of the thermal spray market. However, better control is needed for this process to be used for applications of high precision coatings. This study is aimed at investigating the liquid-metal droplet formation process in order to identify methods for droplet trajectory control. A high speed Kodak imaging system has been used to observe the droplet formation for different operating conditions. Decreasing the upstream pressure and the current levels leads to a reduction in the asymmetric melting of both the anode and cathode. By decreasing the interactions of the large eddy structures with the formed metal agglomerates, one can achieve better control of the particle trajectories and jet divergence. Thus, coatings can be obtained with higher definition and improved reliability.

Keywords atomization, fluid dynamics, melting, thermal plasmas, wire arc

1. Introduction

Much of the investigations concerning the wire-arc spraying process have been directed at correlating process parameters with coating properties while treating the intermediate process of droplet formation as a black box. Few efforts have been directed at understanding the initial stages of melting and particle formation. Observation of the asymmetric melting behavior of the electrodes has been reported.^[1-3] Even fewer researchers have attempted to model the droplet formation and trajectories in the wire-arc spray process.^[4]

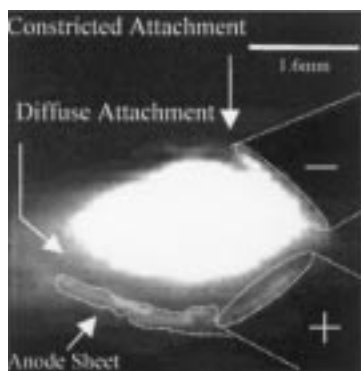
However, a significant amount of research has been performed in the areas of liquid droplet formation, atomization, and particle dispersion in round jets and shear layer flows. Liquid atomization and particle generation have been studied for over a century, dating back to Lord Rayleigh's 1878 work on liquid jet breakup.^[5] Many numerical equations to predict the formed mean droplet sizes have been formulated.^[6] Although the fundamental physical mechanisms of liquid breakup (jets or sheets) into drops have not been established, there seems to be an agreement that the important factors are fluid properties (viscosity, surface tension, and density, although there has been conflicting evidence to the extent of their influence), the relative velocity between the liquid and the atomizing gas, turbulence, and flow separation.^[7] In general, liquid break up occurs with the initiation of a disturbance on the liquid surface, which is enhanced by aerodynamic forces, leading to the formation of ligaments, which may breakup into drops. These drops may also be further broken up into smaller drops (secondary atomization). This is a somewhat simplified but classical picture of the drop formation presented by Dombrowski and Johns.^[8] However, there are major

differences between conventional liquid atomization and liquid metal atomization: (1) the necessity of heating and melting of the metal (which is then atomized) and the means by which it is accomplished, and (2) the different material properties of the metals compared to the liquids (*i.e.*, water) used in conventional atomization processes. The atomization in the wire-arc spraying process might have many factors in common with spray forming and metal-powder production processes, yet it remains distinctly different since the liquid metal is not delivered in a continuous stream in the form of jets or sheets coflowing with the atomizing media (liquid or gas).^[9]

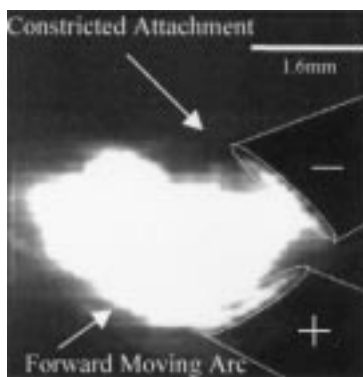
Particle-fluid dynamic interactions require the understanding of the fluid structures, instabilities in the jet, and their subsequent effect on the particles/droplets traversing this jet. Since the introduction of stroboscopic illumination for flow visualization by Rayleigh in 1884 and his first study on jet instability in 1879 (*cf.* Ref 10), a large number of analytical and experimental studies have been undertaken. Two jet instability modes have been observed: (1) a varicose instability characterized by an axisymmetric structure (vortex rings) brought on by Kelvin-Helmholtz instability, and (2) a sinuous instability characterized by helical (spiral) modes of the jet column (which appear as a rhythmic undulation or twisting in the jet).^[11,12] The interaction of jet instabilities with particles in a two-phase flow has been well documented.^[13,14] These studies provided convincing evidence that large scale structures rather than gradient diffusion are the dominant mechanism for particle dispersion. Instantaneous images in particle-laden acoustically forced jets show particles clustering in the high strain regions downstream of vortex rings and a void of particles in the high vortices regions. Thus, particle motion control may be achieved by controlling turbulent structure.

In this study, investigations are reported of the initial stages of metal detachment from the wire tips and subsequent particle formation and interaction with the jet structures. The aim of these investigations has been to generate a basis for fluid dynamic design of a torch, which provides improved particle trajectory and coating quality. We first describe the experimental setup and then discuss the results in three categories: (1) the drop

N.A. Hussary and J.V.R. Heberlein, Department of Mechanical Engineering, University of Minnesota, Minneapolis, MN 55455. Contact e-mail: nah@me.umn.edu.



(a)



(b)

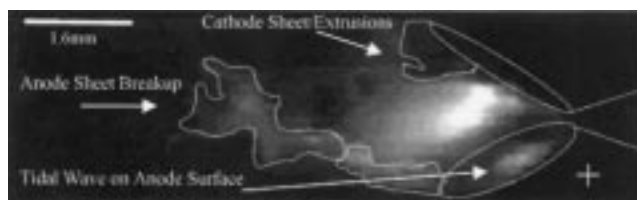
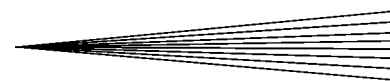
Fig. 1 Diffuse and constricted attachments of the anode and the cathode. The top wire is the cathode and the bottom one is the anode. (a) The arc is fully extended and attached diffusely to the extended anode sheet. (b) The diffuse attachment of the anode is moving forward from the wire tip to the anode sheet ($f = 13,500$ frames/s, $V = 30$ V, $I = 100$ A, and $P = 138$ kPa (20 psi))

formation from the cathode and anode and their effect on particle jet characteristics, (2) the effect of atomization gas pressure and heat input on formed metal sheets and detached ligaments and droplets, and (3) the fluid dynamic interactions with the metal during sheet formation and disintegration and secondary particle breakup.

2. Experimental Setup

A commercial BP400 Praxair Arc Spray System (Praxair Surface Technologies, Appleton, WI) has been used in this investigation. This system consists of a Mogularc 400R power source, a PF400R wire feed unit, and a BP400 gun head. A standard commercial nozzle has been used as well as a previously developed de Laval nozzle.^[15] Nitrogen atomizing gas and carbon steel wire (0.37 to 0.44% carbon and 1.6 mm wire diameter) have been used in all experiments. The angle between the two wires is 30° . The atomizing gas pressure (P) is the measured pressure at the back of the gun head.

A high speed camera (Kodak Ektapro HS Motion Analyzer, Model 4540, Eastman Kodak Company, San Diego, CA), capable of up to 40,500 frames/s, has been used along with a high-magnification Questar Surveillance SZ90 system to view the



(a)



(b)

Fig. 2 The wave on the anode carries the molten metal on the concave anode surface to create the anode sheet at the wire tip. (a) Taken at time $t = 0$. (b) Taken five frames later at $t = 0.28$ ms ($f = 18,000$ frames/s, $V = 30$ V, $I = 100$ A, and $P = 138$ kPa (20 psi))

detachment mechanisms from the wire tips. The high-speed image sequences have then been imported onto a standard video-cassette. A number of filters have been used to reduce the high intensity light from the arc, and a high intensity halogen lamp has been used for back lighting to enhance the contrast on the resulting images.

3. Results and Discussion

3.1 Melting Behavior and Metal Detachment

Asymmetric melting of the wire tips is an inherent feature of the wire-arc melting process since the heating of the anode wire is different from that of the cathode. Figure 1 clearly shows the arc between the two electrodes and the distinct difference between the two arc attachments. The arc attachment on the cathode is constricted while that of the anode is diffuse. Because of these two different arc attachments, the heating, melting, and drop formation from the two electrodes are very different, resulting in a varied range of particle sizes, speeds, and trajectories.

In the case of the anode, the diffuse arc attachment heats a large part of the wire surface, creating a small layer of molten metal on the wire. The atomizing gas stream pushes the molten metal layer, creating a wave that carries the metal to the edge of the wire tip to create the anode sheet, as seen in Fig. 2. The diffuse anode attachment tends to move downstream spreading itself to the continually stretching anode sheet. As the anode sheet breaks away, the arc extinguishes and reignites at the point of closest distance between the electrodes. This cyclic behavior is translated into the familiar fluctuation of the voltage traces. It is also observed that the arc may extinguish without the breaking of the anode sheet but purely due to the aerodynamic forces.

In the case of the cathode, the metal detachment seems to form by three different mechanisms. (1) Ejection of the molten metal as droplets into the cathode jet, as seen in Fig. 3. Due to the variation of the current carrying cross section of the arc (constricted cathode attachment), the interaction of the arc with its

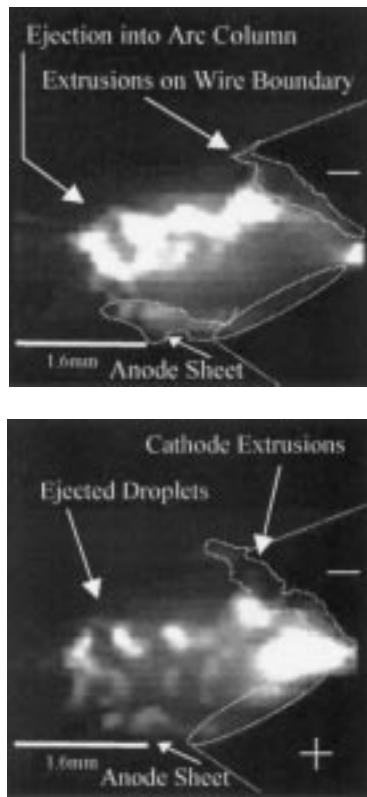


Fig. 3 Ejection of the particles from the cathode into the arc column: two consecutive frames ($f = 13,500$ frames/s, $V = 30$ V, $I = 100$ A, and $P = 138$ kPa (20 psi))

own magnetic field leads to a pumping action and ejection of molten metal into the arc column.^[16] (2) Formation of small extrusions on the wire boundary/circumference that disintegrate before forming a sheet. Often these extrusions are part of a continuous molten-metal ring (or a skirt) around the wire. The constricted arc attachment is observed to move on the cathode surface. The pressure gradient on the wire surface, from the ion jet impinging on the cathode constricted spot, causes the molten metal to be pushed to the wire perimeter creating the metal extrusions.^[17] (3) The small extrusions coalesce to form a cathode sheet on the upper edge of the wire similar to that of the anode but usually smaller in size.

Decreasing the sheet length formed at the anode would accomplish the following: (1) minimize the need for secondary atomization further downstream from the nozzle exit and concentrate the drop atomization close to the gas nozzle exit where the gas jet velocity has not yet significantly declined; and (2) minimize the difference in the initial melting behavior and atomization of the two electrodes to create a narrower particle size distribution, which enhances the potential of fluid dynamic control of the particle's trajectories.

3.2 Atomization Gas Pressure

The effect of the pressure on the arc and the melting of the wire has been investigated by keeping the current and voltage constant and varying the pressure from 138 to 414 kPa (20 to 60

psi). Two distinct effects have been observed. (1) As one might expect, and as has been shown by other researchers,^[2,3] the frequency of the voltage fluctuations increases, as observed in the power spectrum of the voltage trace. The cause of this has been observed, in the high-speed images, to be an increased movement of the arc. The residence time of the arc in a stable position has decreased, and the frequency of the reignition has increased. (2) The melting behavior of both the cathode and the anode changed. In the case of the anode, the increased pressure of the gas leads to the creation of a bubblelike agglomeration of the metal at the end of the anode wire tip (compare Fig. 4a and b with c). This bubble keeps increasing in size, due to the continuous sweeping of the molten metal from the top layer of the wire by the gas, until a critical mass is reached, at which point, this molten globe of mass is stretched out into a long sheet and disintegrates (Fig. 4d). However, at a certain point, when the surface tension force in the sheet becomes stronger than the aerodynamic shear force, the stretched-out anode sheet is contracted back to the wire tip to restart the globe formation. This effect seems to be maximized at an intermediate pressure (345 kPa or 50 psi) with the converging orifice of a standard commercial cap. At higher pressures (414 kPa or 60 psi), the bubble decreases in size, and the contraction of the stretched sheet is almost eliminated (Fig. 4e and f). These effects are attributed to the increase of the aerodynamic forces compared to the surface tension forces. In the case of the cathode, the extrusions that are formed on the wire perimeter seem to increase in size and often join to create a cathode sheet, which does not occur at low pressures. However, the length of this sheet is still shorter than that of the anode. At even higher pressures, the molten material of the cathode tip also becomes more elongated, and a cathode sheet is formed. This sheet seems to be comparable in size to that at the anode. These effects can be seen when comparing Fig. 4(a) and (b) with (e) and (f). It should be noted that the formation of elongated sheets can also be observed when the atomizing gas velocity of the wire tips is increased by changing the shape of the nozzle rather than the pressure, *e.g.*, when using a converging-diverging nozzle.

Control over the melting mechanism of both electrodes can be achieved by using low gas pressure (low jet velocity), which will keep the anode sheet length to a minimum and the cathode atomization process without sheet formation.

3.3 Current Levels—Power Input

The power input into the system is critical in characterizing the melting of the metal and the heating of the atomization gas. The length of the anode sheet increases dramatically from 1/10 the diameter of the wire at a current of 50 A to 2 to 3 times the wire diameter at current levels of 200 A (the pressure is held constant at 138 kPa (20 psi)). The cathode extrusions, which are very small at low currents, increase in size and coalesce to form a sheet that is equivalent to that of the anode. Thus, at high power input levels, both the anode and cathode sheets break up in a similar manner. Therefore, low to intermediate currents should be used to control sheet length on the anode and cathode.

3.4 Fluid Dynamic Interactions

The interaction of the atomizing gas with the wire tip and with the molten metal sheets or the molten metal droplets is com-

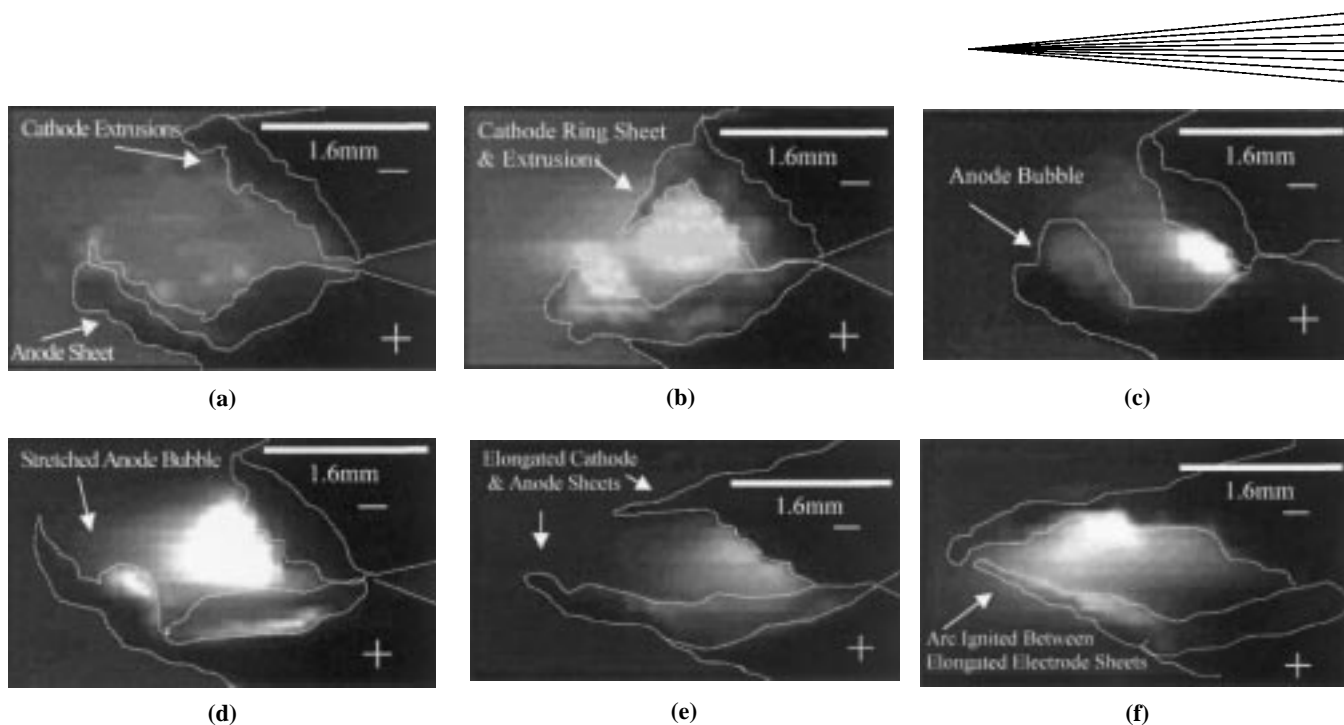


Fig. 4 Effect of upstream pressure on anode and cathode melting behaviors (images taken at 27,000 frames/s). (a) and (b) Anode sheet and extrusions on the cathode perimeter (207 kPa (30 psi), 30 volts, 100 A). (c) and (d) Anode sheet forms a bubble at its tip, which is stretched into a sheet when reaching a critical size (345 kPa (50 psi), 30 volts, 100 A). (e) and (f) More elongated sheets on both electrodes due to increased pressure (414 kPa (60 psi), 30 volts, 100 A)

plex. However, a qualitative analysis of simplified flow patterns may give insight into the physics of the interaction. The discussion will be in three main categories: (1) the fluid structures and interactions that exist in the gas jet, (2) the primary atomization that results from the interaction of the molten metal with the fluid, and (3) the secondary atomization of the droplets and their interaction with the fluid.

The flow in the wire-arc spray process can be simplified as a flow around an obstacle. The two wires and the arc spanning the gap between them can be assumed to be a cylinder in cross flow. The flow around a cylinder is a classical well-documented problem. Figure 5 shows the various flow patterns that arise for varying Reynolds numbers of the flow. To determine the instabilities that might perturb the jet, an estimate of the Reynolds number in the wire arc process is needed. However, the Reynolds number may vary from a few hundred to a few hundred thousand depending on the estimated values of the temperature (thus density and viscosity) and velocity at the exit of the jet. It is safe to say that a complex structure would result from the interaction of (1) the large eddies (vortex street) due to the wake behind the arc and wires, (2) the axisymmetric shear-layer vortex rings at the ambient jet boundary, and (3) possible helical instability in the jet column. The extent of the dominance of any of those modes and the nature of their interactions are yet undetermined. Petersen *et al.* report that axisymmetric structures, or vortex rings, are usually dominant up to $x/D = 4$ (where x is the axial distance from nozzle exit, and D is the jet exit diameter). Beyond the jet core, helical instabilities have a stronger growth rate so that organized helical structures may become important.^[18]

Some of these flow structures have been observed to dramatically influence the primary atomization of the liquid metal. The existence of a pair of vortices fixed in the flow, for example, has been observed by the backward movements of particles trapped

in the wake ($P = 276$ kPa (40 psi), $V = 30$ V, and $I = 100$ A). Large eddy structures in the flow field have also been observed by noting the movement of the anode and cathode sheets, as seen in Fig. 6. These images were taken at 27,000 frames/s. Although these images are not consecutive frames, they demonstrate the formation process of the molten sheet structure. As the sheet starts to extend to a certain critical length, the aerodynamic effect on the movement of the sheet increases by producing bends in the sheet. These bends increase in size as they are carried downstream and further turn with the large eddy structure of the flow. The anode and the cathode sheets then curl a number of times in the flow leading to the structures seen in Fig. 6. As the flapping movement and bending of the liquid metal sheet continues, a critical point is reached at which the surface cannot hold the bending shapes of the metal, resulting in the formation of showers of droplets. The trajectories of those particles are highly dependent on the final sheet position at which the particles form. At the initial stage of formation, the particles possess little momentum. Therefore, the change in the trajectories of these particles by the large eddy structures in the flow is a significant contributor to the spreading of the jet, as seen by the four consecutive frames in Fig. 7.

Secondary atomization of the liquid metal is important in the wire arc process. The well-documented bag-mode drop atomization has been observed in our experiments.^[19] The liquid metal droplets form a balloonlike shape and disintegrate into smaller droplets that spread in a conelike manner leading to spreading of the particle jet. The spreading of the particle jet, therefore, is not only caused by the atomization of the liquid metal sheets but also by the secondary breakup of large drops. Atomized liquid droplets also interact with the large eddy structure in the flow in a similar manner as the liquid metal sheets. Other studies on particle dispersion in a seeded jet that

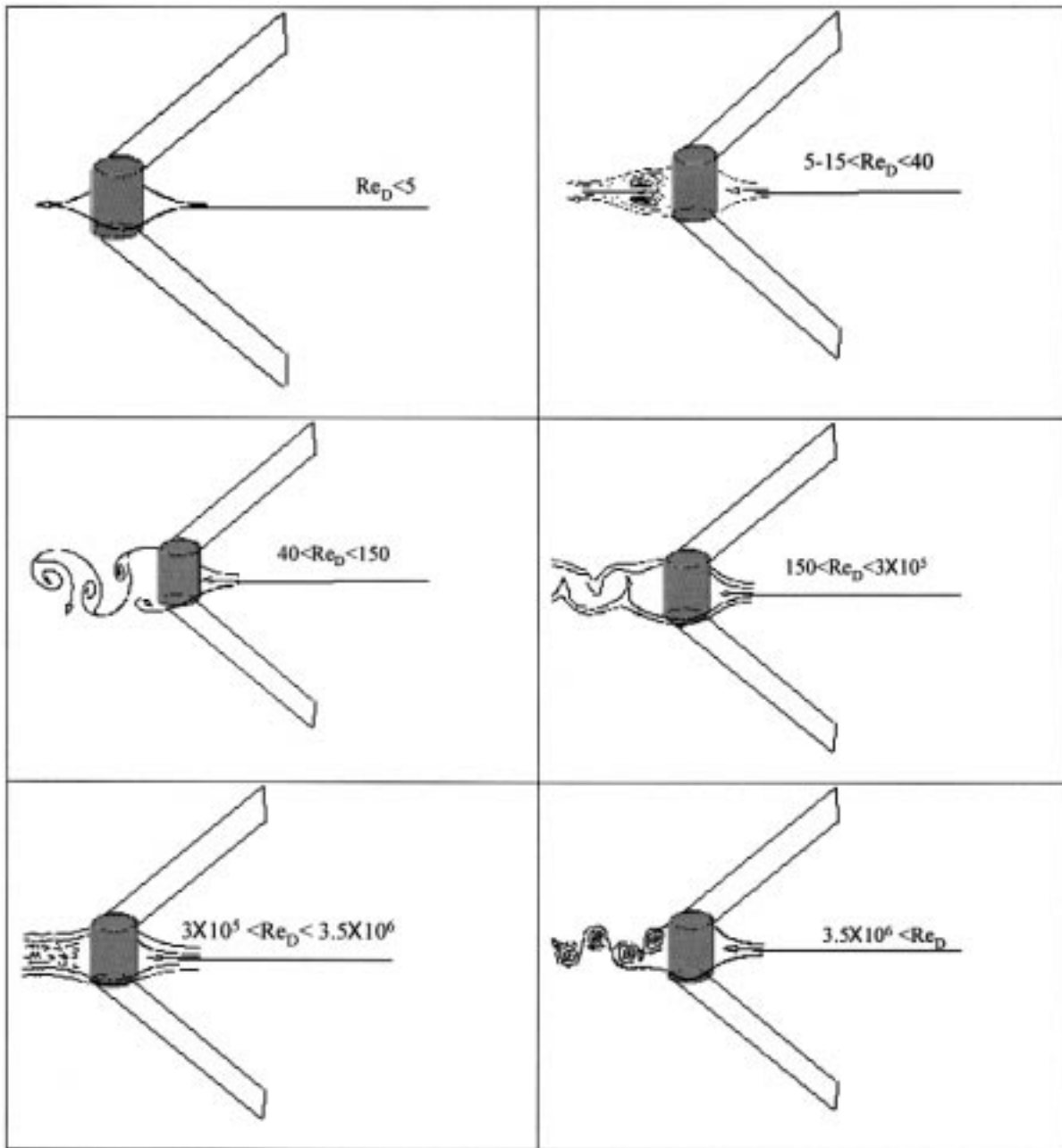


Fig. 5 Main flow regimes for flow across a cylinder (modified by permission of Sparrow^[20])

is forced acoustically to generate strong axisymmetric-vortex rings show clustering of particles as a result of these large flow structures. It was reported that the particle clusters, under appropriate conditions, have an arrowhead shape pointed in the flow direction with tails on the upstream ends that are the result of particles being thrown out of the jet axis. In the wire arc process, a clustering of the molten droplets also occurs (Fig. 8). However, the cause for this clustering may be attributed to two reasons: (1) the intermittent melting and particle detachment of the metal due to arc fluctuations, as shown by Sheard,^[3] although the high speed images in this study reveal less intermittent metal detachment in comparison with Sheard's

conclusions; and (2) the interactions of the particles with the large axisymmetric vortices. The particle interactions with the large axisymmetric vortices are more pronounced when the ratio of the particle inertial time scale to the fluid eddy time scale is around one (Stokes number = 1).

Therefore, minimizing the sheet length and minimizing the secondary breakup further downstream from the gas nozzle exit will decrease the spreading of the particle jet and allow better control of trajectories of slower moving particles. Additional aerodynamic manipulation of the particles can be used to enhance their velocity and alter their trajectories.^[15] Although turbulent flow enhances the breakup mechanism of the molten

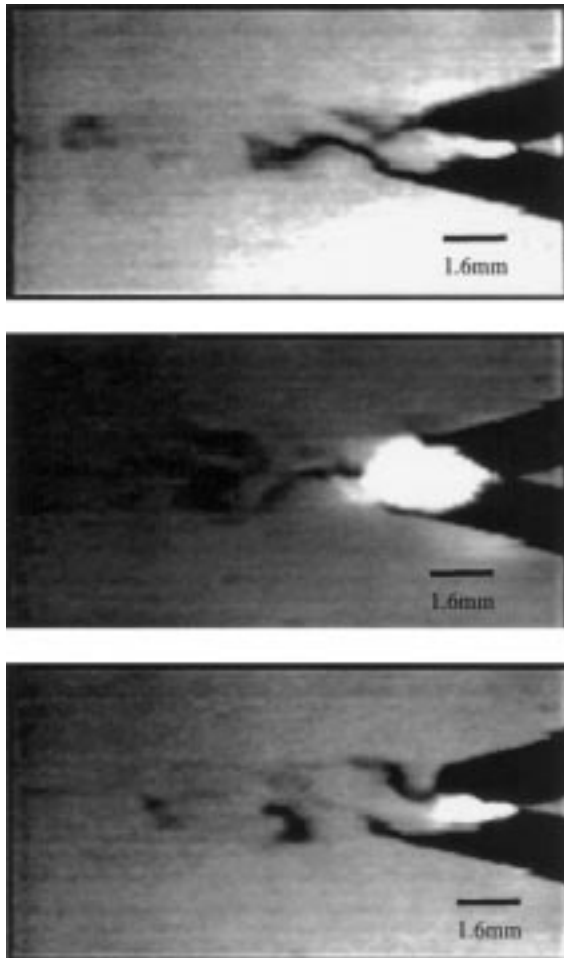
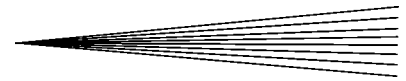


Fig. 6 Large structures in the molten sheets created on both the anode and cathode ($P = 138$ kPa (20 psi), $V = 30$ V, $I = 150$ A, and images taken at 27,000 frames/s)

metal, the large eddy-structure interactions with the molten metal droplets and ligaments can be detrimental to the control of particle trajectories. Therefore, new techniques and designs are needed to minimize large scale eddies while maintaining small turbulent structures.

4. Conclusions

The different mechanisms that govern the metal detachment from the electrodes have significant effects on particle trajectories and jet divergence. The aim of this study has been to develop an understanding of these mechanisms and their effects to improve the control of the process. By using lower atomizing gas pressures and lower current levels (contrary to the levels one is accustomed to in this process), one can decrease the length of the anode sheet and limit the melting and detachment of the metal by means of extrusions on the cathode circumference. Better control of the droplet trajectories can be achieved by minimizing the interactions of the large eddy structures with the created liquid metal sheets to minimize their flapping movement and reduce the divergence of the particle jet. This also reduces the sec-

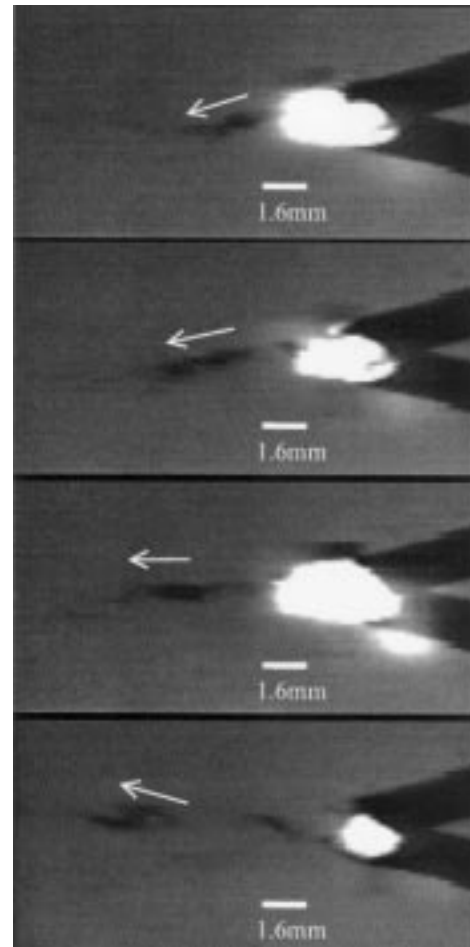


Fig. 7 Consecutive frames showing the abrupt change in the trajectory of the molten metal agglomerates due to the large eddy structures in the flow ($P = 276$ kPa (40 psi), $V = 30$ V, $I = 100$ A, and images taken at 27,000 frames/s)



Fig. 8 Photograph taken with a 35 mm film of the particle jet in the wire arc process

ondary atomization needed further downstream from the gas nozzle exit where the gas jet velocity is significantly lower. To a certain degree, the forces responsible for smaller particle sizes and denser coatings are also responsible for jet divergence. Independent control of particle size and spray pattern requires the separation of the droplet formation from the droplet acceleration, requiring innovative developments in the wire-arc spray process.

Acknowledgments

This work was funded, in part, by Ford Motor Company.

References

1. H.D. Steffens: *Br. Welding J.*, 1966, vol. 13 (10), pp. 597-605.
2. X. Wang: Ph.D. Thesis, University of Minnesota, Minneapolis, MN, 1996.
3. J.S. Sheard: Master's Thesis, University of Minnesota, Minneapolis, MN, 1997.
4. M. Kelkar: Ph.D. Thesis, University of Minnesota, Minneapolis, MN, 1998.
5. L. Rayleigh: *Proc. London Math. Soc.*, 1878, vol. 10 (4), pp. 4-13.
6. A. Lefebvre: *Prog. Energy Combust. Sci.*, 1980, vol. 6, pp. 233-61.
7. N.A. Chigier: *Proc. ICLASS-91*, Hratch G. Semerjian, ed., NIST, Gaithersburg, MD, 1991, pp. 1-15.
8. N. Dombrowski and W.R. Johns: *Chem. Eng. Sci.*, 1963, vol. 18, pp. 203-14.
9. K. Bauckhage: *Proc. ICLASS-91*, Hratch G. Semerjian, ed., NIST, Gaithersburg, MD, 1991, pp. 33-48.
10. H.A. Becker and T.A. Massaro: *J. Fluid Mech.*, 1968, vol. 31, pp. 435-54.
11. S.C. Crow and F.H. Champagne: *J. Fluid Mech.*, 1971, vol. 48, pp. 547-91.
12. A.L. Yule: *J. Fluid Mech.*, 1978, vol. 89, pp. 413-32.
13. B.J. Lazaro and J.C. Lasheras: *Phys. Fluids*, 1989, vol. 1 (6), pp. 1035-44.
14. E.K. Longmire and J.K. Eaton: *J. Fluid Mech.*, 1992, vol. 236, pp. 217-57.
15. N.A. Hussary, J. Schein, and J.V.R. Heberlein: *United Thermal Spray Conf.*, E. Lugscheider and P.A. Kammer, eds., ASM Thermal Spray Society, Dusseldorf, Germany, 1999, pp. 335-39.
16. M. Boulos, P. Fauchais, and P. Pfender: *Thermal Plasmas: Fundamentals and Applications*, Plenum Press, New York, NY, 1994.
17. F. Yin: Master's Thesis, University of Minnesota, Minneapolis, MN, 1999.
18. R.A. Petersen and M.M. Samet: *J. Fluid Mech.*, 1988, vol. 194, pp. 153-73.
19. S.A. Krzeczowski: *Int. J. Multiphase Flow*, 1980, vol. 6, pp. 227-39.
20. E. Sparrow: Lecture Notes, University of Minnesota, Minneapolis, MN, 1997.